TECHNICAL REPORT No. 27

THE ENERGY BUDGETS IN NORTH AMERICA, NORTH ATLANTIC AND EUROPE BASED ON ECMWF ANALYSES AND FORECASTS

by

H. Savijärvi

ECMWF
LIBRARY
26 NOV 1981
No. 1399

November 1981

C O N T E N T S PAGE

ABSTRACT

The kinetic energy, sensible heat and latent heat budgets and the total energy balance at the earth-atmosphere system are studied over North America, North Atlantic and Europe. The data consist of one year (December 1979 - November 1980) of ECMWF initialized objective grid point σ-coordinate analyses and the ensemble of forecasts for day 3.

The results confirm quantitatively the direct meridional circulation over North America with generation of kinetic energy and adiabatic heating in sinking motion; both kinetic energy and sensible heat are exported in the troposphere out of the region. The opposite holds for the North Atlantic area. The residuals of the energy budgets give a realistic approximation of the non-resolved sub grid scale processes (friction, diabatic heating, moisture sources/sinks) in the analyzed data. Budgets from the forecast data reproduce the main features present in the analyzed data but also indicate enhanced vertical motions and some defects in the parameterization of the sub grid scale processes in the model.

The analyzed data, taking 4 analyses per day separately, exhibit diurnal variations, which seem to fit with the observed small diurnal wind. The total energy balance points out to a considerable heat convergence in the North Atlantic ocean.

1. INTRODUCTION

The main purpose of this study is to present internally consistent areal energy budget calculations for some limited areas. Such calculations have been done previously by, e.g. Kung (1967) and Holopainen et al (1978) for kinetic energy and Hutchings (1957) and Rasmusson (1968) for humidity, using aerological observations. The present calculations are based on objectively analyzed grid point data, which has been subject to normal mode initialization. This procedure was preferred to using raw upper air data so as to get a consistent data set; moreover, the advantageous properties of the staggered grid and conservative finite difference schemes originally developed for the ECMWF model could thus be employed for diagnostic purposes.

The vertical profiles of kinetic energy, sensible heat, latent heat and geopotential energy flux convergences and energy conversion terms are studied for three areas: North America, North Atlantic and Europe. The residuals needed for balance in the energy budgets give an estimate of sub grid scale effects (dissipation, diabatic heating, moisture sources) with a space scale separation clearly defined by the grid size. One year of data (December 1979 - November 1980) is used, and the separation of analyses at 0,6,12,18 GMT gives the possibility of finding the thermal tide in the energetics. Results are also shown for the ECMWF numerical forecasts for day 3. The residual in the forecast data is due to the parameterization of sub grid scale effects in the model and its deviation from analyzed data residual points out defects in the parameterization scheme.

All the calculations are for area- and time-averaged values, so no partition into time-mean and transient eddy modes or area mean and deviations has been made. A brief presentation for the winter period only was given in Savijärvi (1980). The analysis system is briefly described in Section 2, the ECMWF model performance for medium-range weather forecasts was described by Hollingsworth et al (1980) and some general circulation experiments with this model were presented in Tiedtke (1980).

2. OUTLINE OF THE DATA-ASSIMILATION PROCEDURE

We give here a short outline of the analysis-initialization procedure, through which the observations were channelled in ECMWF in 1980. The ECMWF operational analyses are made in a 6 hour data assimilation cycle handling observations within $\pm$ 3 hours as simultaneous, the shortest cut-off time being about 8 hours (for the 12 GMT observations). The background field for the analysis is provided by the ECMWF model 6 hour forecast, except above 50 mb persistence

and climatology is used instead. The deviations of observations from the background fields (increments) are analysed in 15 pressure levels with a 3-dimensional multivariate optimum interpolation scheme which uses all the available GTS data including satellite information. The wind increments are, furthermore, subject to local nondivergence within each analysis subvolume (6^{o} x 6^{o} rectangular) and are kept in an approximate geostrophic balance with height increments in the extratropics. The wind divergence is thus due partly to the divergence in the increments on scales larger than about 1000 km. The analysis scheme is described in more detail in Lorenc (1981).

In addition to the analysis of height and wind, a separate analysis of humidity is made. The analysed variable is the integrated water content enclosed between successive standard pressure levels. As with height and wind, the preceding 6 hour forecast is used to provide a first guess field, with appropriate interpolations between pressure and σ-levels. The humidity analysis method uses a single weighted average technique which resembles optimum interpolation for each individual "datum".

In the nonlinear adiabatic normal mode initialization (Temperton and Williamson, 1979) the fields are interpolated to the ECMWF model grid on σ-levels and the time tendencies of the normal modes corresponding to fast gravity waves excited by running one time step of the adiabatic model are removed; the slow Rossby modes are preserved in the process. Wiin-Nielsen (1980) suggested that this procedure should produce more appropriate and consistent (initial) values of the atmospheric variables, in particular velocity potential and vertical velocity, also useful for diagnostic studies. However, as discussed in Temperton (1980) and Kanamitsu (1980), the adiabatic initialization reduces mean meridional circulation and wind divergence especially in the tropics and thereby zonal means of meridional and vertical transports are underestimated. On the other hand, the nonlinear normal mode initialization is capable of producing realistic vertical velocity patterns in midlatitude weather disturbances (Daley, 1980) and subjective inspection of ECMWF analyses suggests that the initialized vertical velocity fields are much more acceptable to a meteorologist than the locally noisy uninitialized vertical velocities. The initialized data should thus be useful for limited area budget studies in midlatitudes.

3. ENERGY BUDGET CALCULATIONS

Kinetic energy, sensible heat and latent heat energy are the only important energy forms for the atmospheric large scale flow. Using sigma coordinates the budget equations for these three energy forms can be written in flux form for a unit mass of air:

$$p_s R_k = \frac{\partial}{\partial t}(p_s k) + \nabla_\sigma \cdot (p_s k \underline{V}) + \frac{\partial}{\partial \sigma}(p_s k \dot{\sigma}) + p_s \underline{V} \cdot (\nabla_\sigma \phi + RT \nabla_\sigma \ell n p_s) \quad (1)$$

$$p_s R_T = \frac{\partial}{\partial t}(p_s C_p T) + \nabla_\sigma \cdot (p_s C_p T \underline{V}) + \frac{\partial}{\partial \sigma}(p_s C_p T \dot{\sigma}) - p_s \alpha \omega \quad (2)$$

$$p_s R_q = \frac{\partial}{\partial t}(p_s L q) + \nabla_\sigma \cdot (p_s L q \underline{V}) + \frac{\partial}{\partial \sigma}(p_s L q \dot{\sigma}) \quad (3)$$

where R_k, R_T, R_q are the net effects (sources) of all contributions not represented by the local change, flux convergences and adiabatic pressure variations. In hydrostatic balance assumed in Eqns. (1) to (4) the adiabatic conversion and generation of kinetic energy through horizontal pressure gradient force are linked diagnostically through geopotential flux convergences ("pressure forces").

$$-p_s \underline{V} \cdot (\nabla_\sigma \phi + RT \nabla_\sigma \ell n p_s) = -\nabla_\sigma \cdot (p_s \phi \underline{V}) - \frac{\partial}{\partial \sigma}(p_s \phi \dot{\sigma} + \phi \sigma \frac{\partial p_s}{\partial t}) - p_s \alpha \omega \quad (4)$$

Here sigma $\sigma = p/p_s$ is the vertical coordinate (pressure normalized by the surface pressure), u, v, $\dot{\sigma} = d\sigma/dt$ are the three wind components, T, q, ϕ the temperature humidity and geopotential, $k = \frac{1}{2}(u^2 + v^2)$ the kinetic energy of horizontal flow, $\alpha = RT/p$ the specific volume and $\omega = dp/dt$. Dividing Eqns. (1) to (4) by g gives the convenient unit of W/m^2 for all the terms.

A comparison between some budget terms calculated in pressure and sigma level coordinates and with and without initialization is given in the Appendix, based on a small sample.

In the following the vertical profiles of the terms in Eqns. (1) to (4) are studied averaged over a one-year period and over three midlatitude areas, determining the right-hand side terms from analyzed (or forecast) wind, temperature and humidity grid point data. The left hand side term (residual) consists then of sub synoptic turbulent flux convergences and other irreversible effects. In particular, R_k is physically the kinetic energy dissipation through surface and internal friction, R_T consists of radiative

effects, latent heat release and turbulent heating and R_q is the net effect of condensation and evaporation and turbulent flux convergences. If forecast data is used in Eqn. (1) to (3), the residual is produced by the subgrid scale parameterization scheme of the particular model; the ECMWF scheme is described in Tiedtke et al (1979).

The finite difference approximations of the energy Eqns.(1) to (4), used in this study are described in Burridge (1980). They are based on the ECMWF adiabatic model equations in a staggered grid, where the wind component points are displaced in regard of temperature points (the Arakawa C-grid). This configuration of variables allows a relatively accurate calculation of divergence and vertical velocity. The relation (4) is accurate in the finite difference scheme, and as the flux divergences disappear in integrating the equations globally with appropriate boundary conditions, this ensures that the finite difference system conserves total atmospheric energy (= potential + kinetic) and moisture in adiabatic conditions (no external sources, i.e. $R_k = R_T = R_q = 0$). (The ECMWF model is actually using equations of motion, where the present difference scheme for rotational terms conserves potential enstrophy in nondivergent flow but does not fully conserve energy). The time change in Eqns. (1) to (3) disappears in the one year time mean of analyzed data except the daily cycle, but not in the forecasts where there may be systematic errors. For the forecasts the time change is calculated as a centred time difference over a 48-hour period.

The vertically integrated continuity equation is in the σ-system

$$\frac{\partial p_s}{\partial t} = - \int_0^1 \nabla_\sigma \cdot (p_s \underline{V}) \, d\sigma \qquad (5)$$

where the boundary conditions $\dot{\sigma} = 0$ at $\sigma = 0$, $\sigma = 1$ have been used. Global mass of the atmosphere is conserved by the adopted difference scheme.

It was found that the ECMWF initialized analyses conserve mass also locally very well, i.e. the time mean vertical integral of mass convergence vanishes at all points (except for the thermal diurnal tide), and no artificial correction for the mass balance, typically encountered with aerological data (O'Brien, 1970), was needed. However, this was not the case with the ECMWF forecast ensemble means, where the systematic error of the model shows up as local surface pressure change of the order of several millibars per day. The pattern of this systematic error is rather similar at all heights (Derome, 1981) and, in accordance with Eqn. (5), excites vertically constant large scale divergence of the order of 10^{-8} s^{-1}. This "spurious" mass diver-

gence is not important in kinetic or latent heat energy budgets but has to be considered for sensible heat.

The data material consists of ECMWF analyses and forecasts for the year December 1979 - November 1980 in a 1.875^{o} geographical grid (N48). As discussed above, initialization reduced mean meridional circulation to a level where zonal parts of transports of temperature, humidity, etc. are strongly underestimated, so the budgets will be discussed only for three limited areas in the northern hemisphere. The areas, shown in Fig. 1, cover North America, North Atlantic and Europe. The area averages shown are weighted sums of the terms calculated in all grid points within the area. For horizontal flux divergences this gives the same result as line integration along the area boundaries (by Gauss theorem) often used in aerological data studies. The analysis-initialization step should make data consistent in that the temperature (geopotential), humidity and horizontal wind all contain only scales representable by the grid, and there is a clear scale separation between large-scale contributions and sub-grid scale, the net effects of which are represented by the residuals R_k, R_T, R_q. This scale separation may be obscured in studies using aerological data.

3.1 Kinetic energy budget

Fig. 2a shows the kinetic energy budget terms (Eqn. 1) for the three areas taking the yearly mean of 4 analyses per day (00, 06, 12, 18 GMT). There are 1414 cases in all. The North American area is similar to the area Kung used in a series of articles on kinetic energy dissipation calculated as a residual from aerological data. The main features and numerical values of the terms in Fig. 2 are, for North America, very similar to Kung and Baker's (1975) annual mean values for 5 years of data.

The upper tropospheric flow over the North American continent is a source of kinetic energy (positive generation) which is then exported horizontally while the North Atlantic and European areas act as sinks for kinetic energy importing the loss from outside. The implied poleward mean ageostrophic wind in the confluent flow over North America and equatorward ageostrophic wind in the jet exit over North Atlantic and Europe is in good agreement with Lau's (1979) work on the maintenance of the time mean flow in winter.

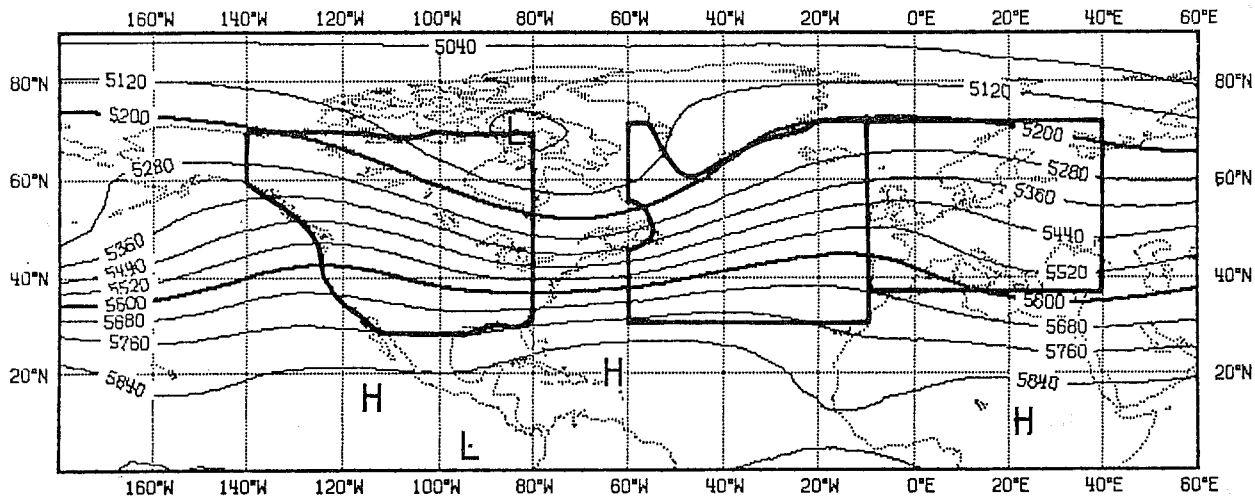

Fig. 1 Normal January 500 mb height contours and the three areas used for energy budget calculations

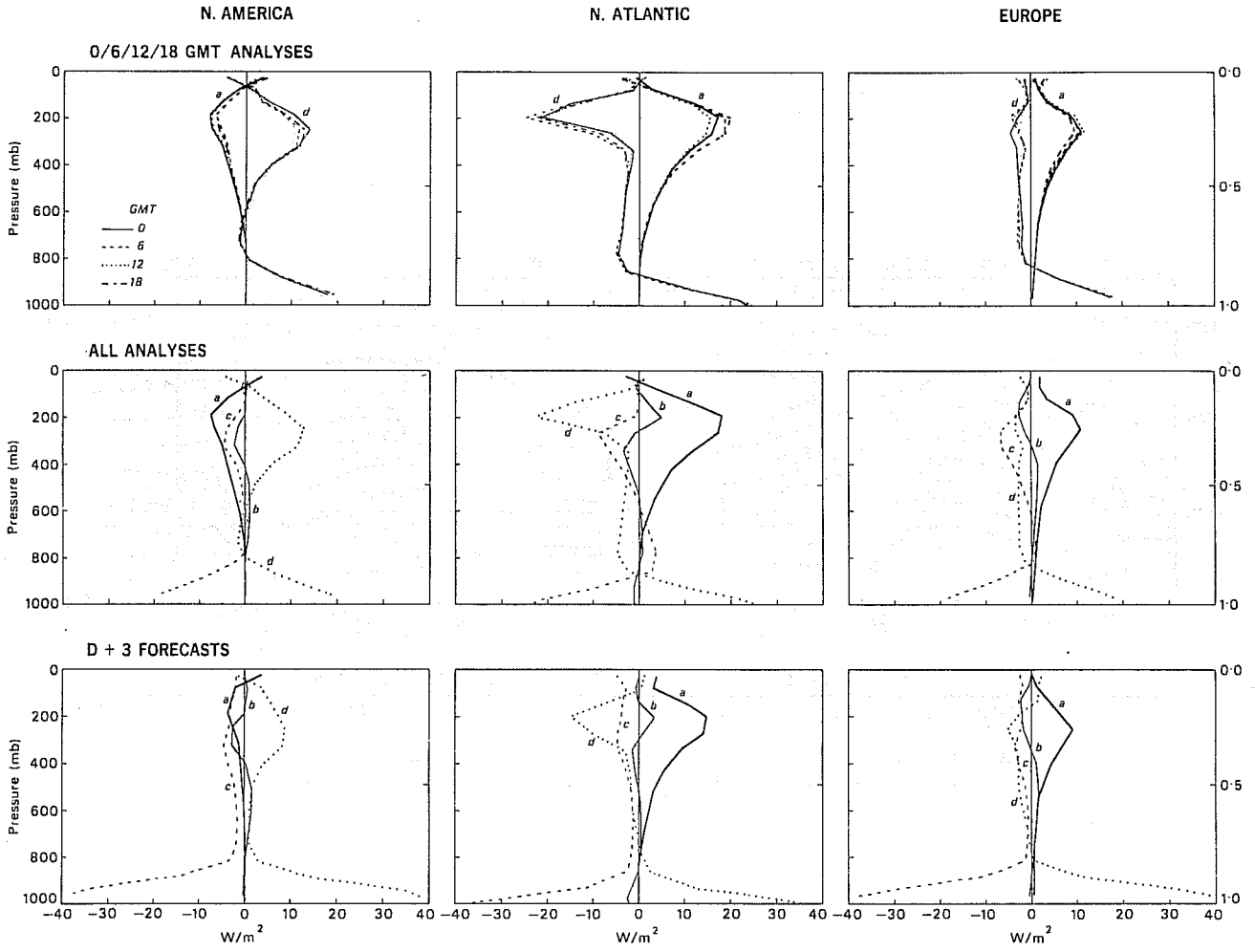

Fig. 2 The kinetic energy budget over North America, North Atlantic and Europe in December 1979-November 1980. Unit: W/m^2.
Top : Initialized ECMWF analyses at 0,6,12,18 GMT
Middle : Average of the four analyses per day
Bottom : ECMWF numerical forecasts valid at day 3

a) horizontal kinetic energy flux convergence

$$-\nabla_\sigma \cdot \overline{(kp_s\underline{V})}/g$$

b) vertical kinetic energy flux convergence

$$-\frac{\partial}{\partial\sigma}\,\overline{(kp_s\dot{\sigma})}/g$$

c) residual $R_k = -(a+b+d)$; estimate of net dissipation by friction

d) kinetic energy generation $-\overline{p_s\underline{V} \cdot (\nabla_\sigma\phi + RT\nabla_\sigma \ell n p_s)}/g$

The residual term shows in all three areas two maxima, in the 300 mb level and in the planetary boundary layer. The unphysical "negative dissipation" in the layer between 700 and 800 mb caused by negative generation term is probably due to the initialization (Savijarvi, 1981); this phenomenon is more severe over ocean areas. The boundary layer dissipation values for the three areas are listed in Table 1 for annual mean and for seasons:

Table 1. Boundary layer (σ<0.845) residual dissipation from ECMWF analyses (W/m^2)

	Year	Spring	Summer	Autumn	Winter
North America	1.5	1.6	1.0	1.6	1.9
North Atlantic	2.2	2.0	1.2	2.6	3.0
Europe	1.6	1.3	1.4	1.8	1.8

The free atmosphere dissipation and its secondary maximum is larger over the Atlantic and European areas than over the North American continent. This agrees with Elsaesser's (1969) results for the turbulent dissipation in the free atmosphere above 850 mb; based on wind variance statistics through Kolmogorov's turbulence theory he obtained area averaged values of 2-3 W/m^2 over Atlantic and 1-2 W/m^2 over North America.

Holopainen and co-authors (1973, 1978, 1979) have studied extensively the kinetic energy budget over Britain and north western Europe using aerological data. A persistent feature in these works has been the large negative kinetic energy generation not completely balanced by horizontal convergence of kinetic energy in the free atmosphere, leading to positive residual values. This energy input from subgrid scales to the synoptic scale is contradictory to the present results. However, Holopainen's results are for a much smaller area. Also Vincent (1981) has suggested that strong convective activity over a small area could lead to such an upscale energy cascade.

The variation in Kung's (1967) results for 0 GMT and 12 GMT data taken separately was suggested by Wallace and Hartranft (1969) to be due to the (diurnal) thermal tide in the atmosphere. Fig. 2b presents the budgets for the ECMWF analyses separated to 0, 6, 12 and 18 GMT annual means. The diurnal variation over North American area is very similar to Kung's findings. Over the North Atlantic area the annual mean of kinetic energy generation is, at the 200 mb level, -25 W/m^2 at 6 GMT analyses and -21 W/m^2 at 12 GMT

analyses. Assuming that the average geopotential gradient is equivalent to a constant westerly geostrophic wind of 20 m/s, this difference would suggest for the meridional wind component $v_{06GMT} - v_{12GMT}$ a value of 20 cm/s southerlies. This value is of the same order as that predicted by tidal theory (Chapman and Lindzen, 1972) for latitude 50°N; for observed lower stratospheric winds over England (100 - 150 mb 8 observations per day) Johnson (1955) reported diurnal southerly winds $v_{06} - v_{12}$ of about 50 cm/s. The adiabatic initialization may, however, reduce the amplitude of the diurnal wind variation, because this variation is driven mainly by the purely diabatic direct absorption of solar radiation in ozone and water vapour through deep layers of the atmosphere.

The variation of the analyzed wind speed within the four analyses per day is about 30 cm/s in the 200 mb level over the three areas. That the systematic diurnal variation can survive initialization at all is interesting because random variations, produced for a Monte Carlo forecast experiment, did not survive (Hollingsworth and Savijarvi, 1980), even if they were set into geostrophic balance with mass variations.

Fig. 2c gives the kinetic energy budgets taking the annual mean of all ECMWF forecasts valid at day 3. There are 285 cases, as forecasts were not made during week ends for large part of 1980. The small local decrease of kinetic energy in all levels in the kinetic energy during the forecast is disregarded in Fig. 2c because it amounts only to about 0.1 W/m^2.

The boundary layer cross-gradient flow, generating kinetic energy, is stronger in the forecasts than in the initialized analyses. This is balancing the dissipation through parameterization of turbulent momentum fluxes with the aid of mixing length theory in the ECMWF model. Initialization might reduce this diabatic dissipation in the analyzed data, but as discussed in Temperton (1980) and Daley (1980), the reduction is probably small for this shallow layer phenomenon. The boundary layer values in observed data studies (Kung et al, 1975, Holopainen, 1979) are, moreover, nearer to the analyzed values than to the 3-day forecasts.

In the free atmosphere all the terms in the kinetic energy budget have smaller values in the forecasts than in the analyzed data. This is probably due to the zonalization of the flow during the forecast. This feature is typical for most atmospheric models and leads to the underestimation of climatological ridges in the ECMWF forecasts with the largest systematic error in wavenumbers 2-3.

3.2 Temperature budget

In the kinetic energy budget the advective part dominates the horizontal and vertical flux divergences locally ($\nabla . (k \underline{V}) \sim \underline{V} . \nabla k$)
In the sensible heat flux divergence the divergent part dominates ($\nabla . c_p T \underline{V} \sim c_p T \nabla . \underline{V}$), and because of the continuity equation, the local horizontal and vertical sensible heat flux divergences tend to be very large but opposite in sign. This is illustrated in Fig. 3 where the terms in the sensible heat flux budget (Eqn. 2) are shown averaged for one year 12 GMT analyses over North America. It is seen that the strong vertical convergence of sensible heat is nearly balanced by strong horizontal divergence out of the area in the lower atmosphere while the reverse is taking place in the upper troposphere. The net effect is a weak divergence of the 3-dimensional heat flux, which is nearly balanced by adiabatic heating through the conversion term $\alpha\omega$, so that the diabatic heating needed for complete balance is indeed a small residual. Comparing the conversion values in Fig. 3 to the kinetic energy generation in Fig. 2 it can be deduced that locally most of the converted total potential energy (sensible heat) goes to keep up pressure forces (Eqn. 4) and only a small amount is actually used to accelerate the flow in the form of kinetic energy generation. The kinetic energy generation is itself largely balanced by horizontal advection of kinetic energy (Fig. 2) so that dissipation remains small. These delicate balances arise from the nearly quasi-geostrophic nature of the large-scale flow in middle latitudes.

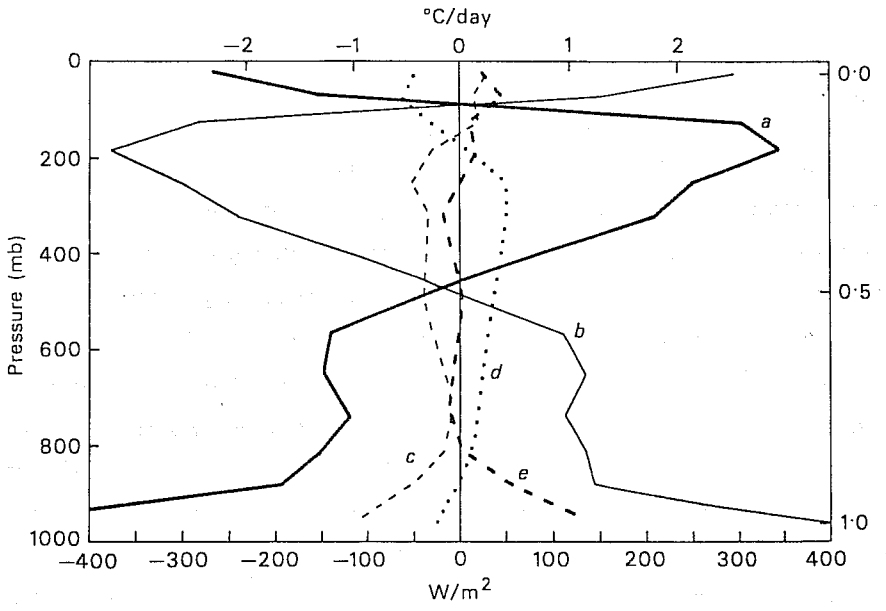

Fig. 3 The time and area averaged sensible heat budget over North America from ECMWF initialized 12 GMT analyses in December 1979-November 1980. Unit: W/m^2; $1^{\circ}C/day \sim 115\ W/m^2$.

a) horizontal heat flux convergence $- \nabla_\sigma \cdot \overline{(c_p T p_s \underline{V})}/g$

b) vertical heat flux convergence $- \frac{\partial}{\partial \sigma} \overline{(c_p T p_s \dot{\sigma})}/g$

c) total heat flux convergence (sum of a and b)

d) energy conversion rate $\overline{p_s \alpha \omega / g}$

e) estimate of diabatic heating $R_T = -(c + d)$

Fig. 4 shows the annual temperature budget for all analyses (4 per day). The horizontal and vertical flux divergences have been combined. In the middle and upper troposphere the continental regions (North America and Europe) in the climatological jet entrance and confluent flow are areas of descending air (adiabatic heating) and sensible heat flux divergence, while the North Atlantic area, over the climatological jet exit, exhibits convergence of heat flux and rising motion. Combined with the kinetic energy considerations the emerging thermally direct meridional circulation in the confluent flow and indirect (Ferrel type) circulation over the jet exit area is coherent with the results of Blackmon et al (1977), Lau (1979) and Savijärvi (1977), all calculated from statistics based on NMC analyses.

In the boundary layer the large-scale flux divergence is accompanied by systematic adiabatic cooling ($\alpha\omega<0$). The latter effect is needed to balance the kinetic energy generation (Eqn. 4) because pressure forces are small near the ground. Another description of this consequence of "Ekman pumping" can be given by writing, in the σ-system

$$p_s \alpha\omega = RT \underline{V} \cdot \nabla p_s - \frac{RT}{\sigma} \int_0^\sigma \nabla_\sigma \cdot (p_s \underline{V}) \, d\sigma \qquad (6)$$

where the continuity equation and boundary conditions $\dot{\sigma} = 0$ at $\sigma = 0$, $\sigma = 1$ have been used. The last term disappears near the ground on the average (because of mass balance requirements), and the first term must produce negative values there because the winds are turned towards lower pressures by friction. The frictional drag is so adjusted that the values of $\alpha\omega$ are nearly the same over the land and sea surface layers in the initialized analyses. This feature is peculiar to the σ-system and is absent in pressure coordinates.

The residual R_T in Fig. 4 represents the net effect of all diabatic heating sources. The values result as a small residual between large divergent-dependent terms (Fig. 3) and the accuracy of R_T is thus very much dependent on the quality of divergent winds in the data. This is effectively demonstrated in Fig. 4b where the annual temperature budget is separated into the four daily analyses. It is suggested that the large daily variation in the individual terms seen in Fig.4b is real and due to the small but systematic divergence of the migrating diurnal wind component. As discussed with the kinetic energy budget, the diurnal wind component may be underestimated in the initialized data and so the variations in the local temperature budget terms may be even larger in reality. Fig. 4b suggests that in temperature budget studies only one observation per day may give locally misleading results.

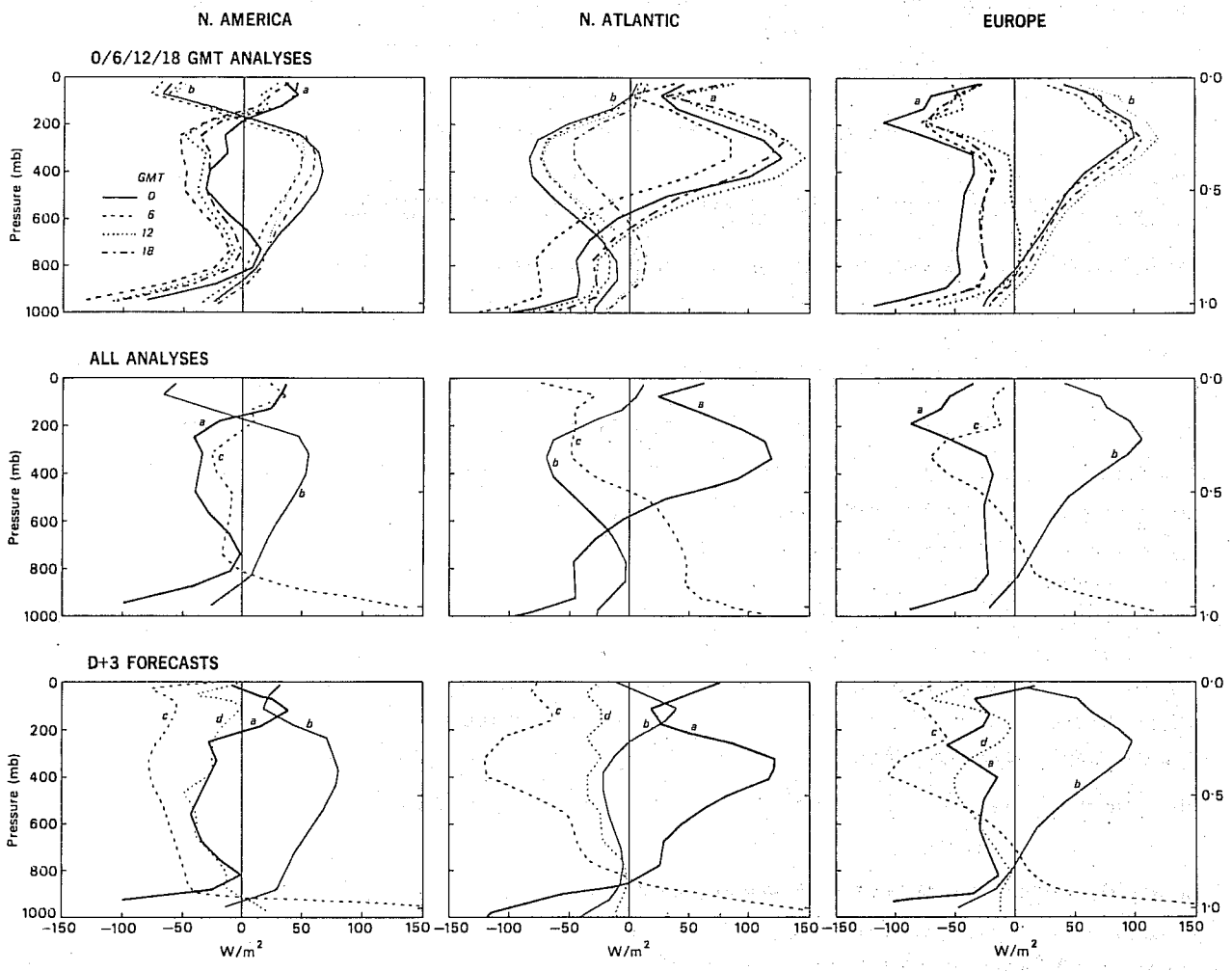

Fig. 4 As Fig. 2 but for the sensible heat budget.
Unit:W/m^2; $1^oC/day \sim 115\ W/m^2$.

a) 3-dimensional heat flux convergence

b) energy conversion rate $\overline{p_s \alpha \omega / g}$

c) residual $R_T = -(a+b+d)$; estimate of net diabatic heating

d) local change $p_s \partial\overline{T}/\partial t$ following the forecasts (negligible in the analysed data)

The residual profile from Fig. 4a, interpreted as net diabatic heating, shows boundary layer heating, which amounts to about 120 W/m^2 or 1^oC/day near the surface in all three areas. Over the ocean area the heating is extended into a deeper layer up to 500 mb, and (radiative) cooling predominates in the upper atmosphere except in the North American stratosphere. These features agree with estimates of diabatic heating by e.g. Lau (1979) and Clapp (1961) for wintertime northern hemisphere, but numerical values are smaller in the present study.

Fig. 4c gives the ensemble mean of the sensible heat budgets calculated from all ECMWF 3 day forecasts for December 1979 - November 1980. The model parameterization did not include the daily cycle.

To make comparison easier the local mass convergence due to the systematic error of the model has been removed. This mass balance correction varies in space and forecast length, but for the day 3 North Atlantic and European areas it is small (equivalent to divergence of less than 5.10^{-8} s^{-1}) as these areas include systematic pressure decreases and increases at about the same amount on the average. Over the North American area the surface pressure is increasing on the average with a rate of 3 mb/day at day 3. The temperature flux divergence corresponding to this local change $c_p \bar{T} \frac{\partial \bar{p}_s}{\partial t}$ is about -100 W/m^2 or -1^oC/day.

A new profile is present in Fig. 4c. This is the local temperature change $c_p \bar{p}_s \partial\bar{T}/\partial t$ in the model, calculated as the area averaged temperature difference between forecast days 4 and 2. There is general cooling in the ECMWF model, which contributes to the systematic error. Comparing the forecast profiles with those from the analyses it can be seen that over the continental areas the agreement is in general good and if the systematic cooling is disregarded, the parameterization of the sub grid scale effects in the ECMWF model is capturing the net diabatic sources. Over the North Atlantic upper troposphere the large temperature flux convergence is balanced mainly by strong (radiative) cooling in the forecast while in the analyzed data the adiabatic cooling ( ) was the main balancing agent. The parameterization of the ECMWF model does not produce the extended heating up to the 500 mb level over the ocean, present in the analyzed data. This indicates relative weakness in condensational processes over the ocean, presumably in the convective (Kuo) scheme during cold outbreaks.

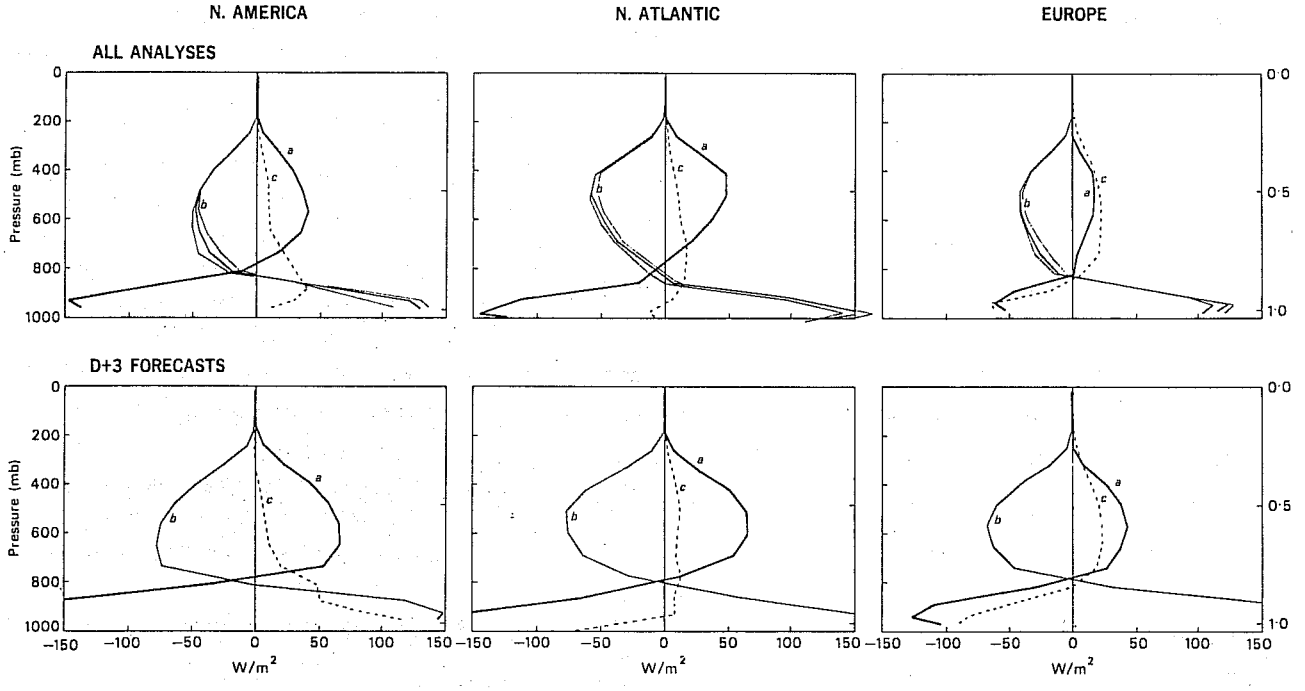

Fig. 5 The latent heat energy budget over North America, North Atlantic and Europe in December 1979 - November 1980.
Unit: W/m^2; 1 mm H_2O/day ~30 W/m^2.

Top: average of four daily analyses. The diurnal deviation around the mean in the residual curve b) is indicated by thin lines.

Bottom: ECMWF numerical forecasts valid at day 3.

a) vertical latent heat flux convergence $-\frac{\partial}{\partial\sigma}\overline{(Lqp_s\dot{\sigma})}/g$

b) residual $R_q = -(a+c)$; estimate of net moisture sources

c) horizontal latent heat flux convergence $-\nabla_\sigma \cdot \overline{(Lqp_s\underline{V})}/g$

3.3 Humidity budget

The humidity (latent heat) budget (Eqn. 3) is rather simple for a long time mean: in each fixed air volume the horizontal and vertical convergences of the time-mean humidity flux must be balanced by net sources or sinks. In grid point data the sources and sinks include the subgrid scale flux convergences in addition to the time-mean condensation and evaporation within the volume. If vertically averaged, these amount to the evaporation minus precipitation on the surface; and this loss (gain) in the total water content in the air column must be balanced by flux convergence (divergence) through the horizontal walls.

Fig. 5 shows the annual mean of the humidity budget averaged over the three areas where the net sources are represented by the residual needed to balance the horizontal and vertical large-scale flux convergences. All the 4 analyses per day are used. The humidity was actually analyzed with the aid of observations only for the winter period (December 1979 - March 1980). During April - November 1980 the initial humidity field, from which the ECMWF model started and which was also used in the present diagnostic calculations, was replaced by the 6 hour forecast for humidity.

The boundary layer is a layer of vertical flux divergence as moisture is transported upward from the surface in large-scale eddies. In mid troposphere all the three areas accumulate moisture by both vertical and horizontal large-scale convergence, which is being removed (negative residual) presumably by condensation. In the boundary layer there is net horizontal inflow of humidity over the North America while the net is small over North Atlantic (large inflow from west, but similarly large outflow in the east) and the European area indicates net horizontal outflow. The large positive residual needed to compensate the flux divergence in the boundary layer is due to evaporation from the surface and in the rainfall, and the net effect of (mainly vertical) convergence of humidity flux in small scale eddies. The four daily analyses are not presented but the small diurnal variation in the residual is shown as the envelope curve made by all four daily analyses. However, the numerical values of humidity flux convergences are probably too small in the initialized data:

Fig. 5 shows the latent heat budgets for ECMWF day 3 forecasts. The moisture content of the model atmosphere is decreasing slightly, presumably due to the cooling, and the locally nonvanishing mass balance due to the systematic error creates also apparent local changes of humidity. Thus $\frac{\partial}{\partial t}(p_s L_q)$ is nonzero. It is, however, only a few W/m^2 for the data in Fig.5 and is disregarded here.

In the middle troposphere the horizontal flux convergence of the forecast is similar to the analyzed but in the boundary layer it is enhanced. The large scale vertical convergence is greatly enhanced through the whole column. This is an illustration of the "spin-up" problem: the (initialized) analysis does not provide intense enough correlation between humidity and vertical velocity, and it takes a few days for a model to reach its own circulation regime (Bengtsson, 1980). Daley (1980) suggests that the humidity analysis should be modified before the numerical short-range precipitation forecasts can be significantly improved. (Recent changes in the ECMWF analysis/ initialization system have virtually removed the spin-up of condensational processes).

Table 2 lists the vertically integrated humidity flux convergences from Fig. 5 converted into cm/year of evaporation minus precipitation over the area.

Table 2. Vertical integral of the humidity flux divergence in cm/year in ECMWF data for December 1979-November 1980.

	All analyses	3 day forecasts
North America	-13.42	-19.73
North Atlantic	- 8.18	- 3.72
Europe	-7.32	- 1.81

Rasmusson (1968) has used aerological data to estimate E-P over USA and South Canada for two one year periods. His results, excess of precipitation of 16.0 and 18.8 cm/year, are near to those obtained here. The diurnal variation (taking 00 and 12 GMT observations separately) in Rasmusson's results was much larger than in the present results.

3.4 Total energy flux divergences

If the energy equations (1-4) are integrated vertically through an atmospheric column, and similarly, energy equations valid for the ocean-soil-cryosphere column are integrated from the surface down to the depth where the fluxes disappear, the sum is the equation for the total energy (Oort and Vonder Haar, 1976):

$$S_A + S_0 = -\nabla \cdot (\underline{F}_A + \underline{F}_0) + R_{ea} \tag{7}$$

of the earth-atmosphere system.

S_A and S_0 are the local rates of change in the vertically integrated energy contents of the atmospheric and "oceanic" column (in the form of sensible heat, latent heat and kinetic energy for the atmospheric column). These storage terms disappear in a long time mean. Then, the time mean horizontal net energy flux divergence $\nabla \cdot (\underline{F}_A + \underline{F}_0)$ must balance the net energy flux R_{ea} through the "vertical boundary"; R_{ea} is physically the net radiation of the earth-atmosphere system at the top of the atmosphere and measurable by satellites. The vertically integrated flux of total atmospheric energy F_A is in σ-coordinates:

$$\underline{F}_A = \int_0^1 (c_p T + Lq + \phi + k)\, p_s \underline{V} \frac{d\sigma}{g} \tag{8}$$

The wind in (8) can be either horizontal or 3-dimensional, because the vertical integration with the boundary conditions $\dot{\sigma} = 0$ at $\sigma = 0$, $\sigma = 1$ gives no net contribution from the vertical flux.

For zonally averaged conditions, e.g. Oort and Vonder Haar (1976) and Newell et al (1974) have discussed the total energy budget. For limited areas there have been very few studies (cf, Alestalo, 1981), because of the large effect of wind divergence in the temperature and geopotential flux divergences and the difficulty to get reasonable divergence values from observed winds.

The present results from ECMWF initialized analyses give a possibility to study the total energy flux divergence $\nabla \cdot \underline{F}_A$ in the atmosphere over the three areas North America, North Atlantic, Europe. The North American area is land, where the horizontal fluxes F_0 through the boundaries must be small, thus the net radiation R_{ea} above this area should equal the atmospheric energy flux divergence in the long run. In the North Atlantic area, the heat flow in the ocean $\nabla \cdot \underline{F}_0$ may be large while the European area is partly land, partly sea.

In Fig. 6a the vertical profiles of the four atmospheric energy flux divergencies are collected together. The divergences are 3-dimensional and the annual mean of initialized analysis calculations (4 analyses per day) is presented.

It can be noted that near the surface the large positive sensible and latent heat divergences dominate the total energy. The kinetic energy flux divergence is relatively small everywhere. In the upper troposphere, the geopotential and sensible heat flux divergences are large but tend to balance each other. In the middle troposphere the latent heat flux convergence gives the largest contribution to the total flux divergence.

Fig. 6b presents the profiles for annual means of individual analysis 0, 6, 12, 18 GMT. The sensitivity of geopotential and sensible heat to wind divergence suggested to originate from diurnal wind is obvious, while the latent heat and kinetic energy flux divergences are less sensitive. (The diurnal wind speed is only about 30 cm/s at the 200 mb level in the data.) This sensitivity and the tendency of balance between the two largest contributions means that the sum $\nabla.\underline{F}_A$ of the vertical integrals of the four flux divergences must be considered with caution.

The annual area averages of the energy budgets are presented in Table 3, integrated vertically, taking the mean of all four analyses per day.

Table 3. Vertically integrated annual energy budgets in W/m^2

Sensible heat budget (Eqn.2)

	$\mathrm{div}(c_p T\underline{V})$	$-\alpha\omega$	sum $\cong$ diabatic heating
Europe	40.0	-46.3	-6.3
North Atlantic	-21.6	+27.5	+5.9
North America	17.9	-15.6	+2.3

Latent heat budget (Eqn.3)

	$\mathrm{div}\,(Lq\underline{V}) \cong L(E-P)$
Europe	-6.1
North Atlantic	-6.7
North America	-11.0

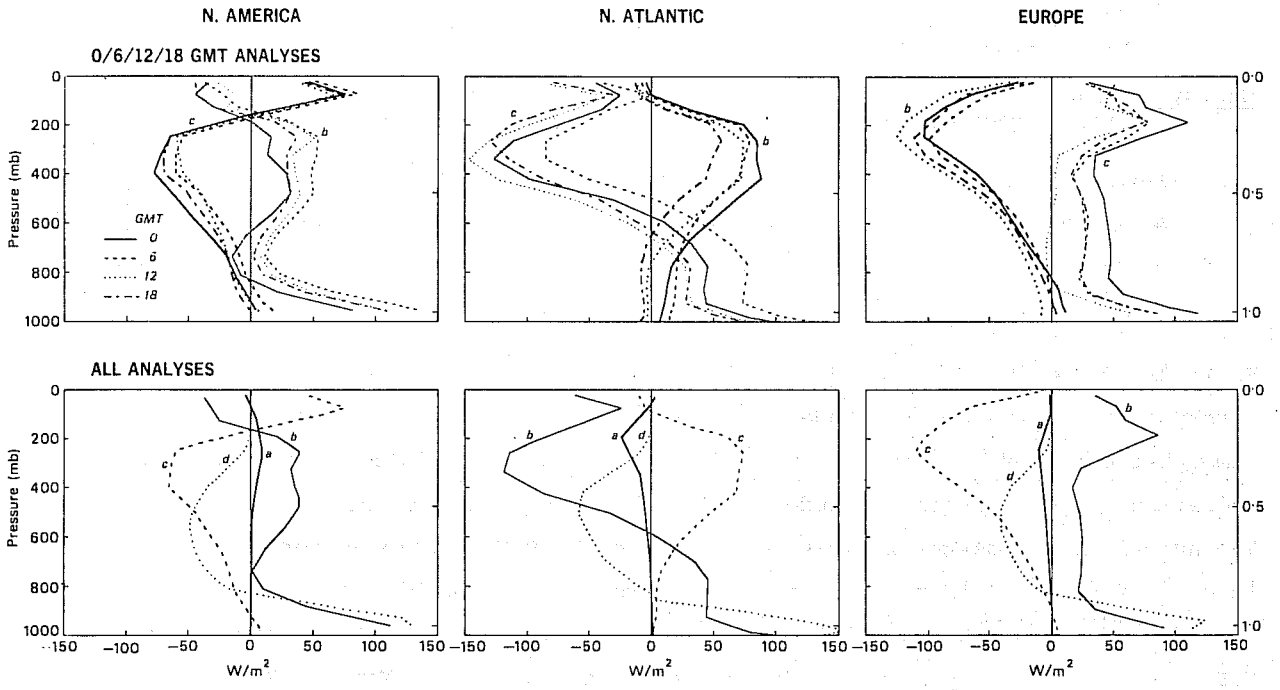

Fig. 6 The atmospheric 3-dimensional energy flux divergence profiles over North America, North Atlantic and Europe in December 1979 - November 1980. Unit: W/m^2.

Top: initialized ECMWF analyses at 0, 6, 12, 18 GMT

Bottom: average of the four daily analyses

a) kinetic energy $\frac{1}{2}\underline{V}^2$

b) sensible heat energy $c_p T$

c) geopotential energy ϕ

d) latent heat energy Lq

Kinetic energy budget (Eqn. 1)

	div($k\underline{V}$)	-generation	sum $\cong$ -dissipation
Europe	-3.6	0.6	-3.0
North Atlantic	-5.3	2.6	-2.7
North America	2.2	-4.5	-2.3

Energy flux divergencies div($s\underline{V}$)

	$S = c_p T$	Lq	ϕ	k	sum = $\nabla.\underline{F}_A$
Europe	40.0	-6.1	-45.7	-3.6	-15.4
North Atlantic	-21.6	-6.7	30.1	-5.3	-3.5
North America	17.9	-11.0	-20.1	+2.2	-11.0

Estimates by Oort and Vonder Haar (1976) for the zonally averaged flux divergences in the mid-latitude belt 30-70° N give -18 w/m^2 for the atmospheric part $\nabla.[\underline{F}_A]$ and -22 w/m^2 for the oceanic part $\nabla.[F_0]$, and the net radiation $[R_{ea}]$ for this latitude belt is about -40 w/m^2 (Lorenz, 1967). The annual total energy flux divergences from the ECMWF analyses for the three limited areas in this latitude belt are thus reasonable, considering the sensitivity of the calculations although the value for North America, $\nabla.\underline{F}_A$ = - 11 W/m^2, is probably underestimated in magnitude. Maps of R_{ea} from satellite measurements (Raschke et al, 1973) indicate that R_{ea} does not vary much longitudinally around the zonal mean (-40 w/m^2) in these areas, so that the oceanic heat flow in the North Atlantic area must be large, because the atmospheric part $\nabla.\underline{F}_A$ is small, -3.5 w/m^2. This area is in the middle of the Gulf Stream so that large convergence of heat flow in the oceanic currents is expected.

Recent studies have stressed the role of oceanic heat transports also for the zonally averaged conditions (Vonder Haar and Oort, 1973). It may eventually be possible to map geographically the atmospheric heat flux divergences and get indirectly the ocean heat divergences with the aid of R_{ea}-measurements. Based on the present results, a good quality divergent wind field is needed for reasonably accurate $\nabla.\underline{F}_A$.

Alestalo (1981) has calculated the total energy flux divergences using European aerological data for 3 years. His results give $\nabla.\underline{F}_A = -55$ w/m² for continental Europe, which is reasonable, but this is arrived at with opposite signs of sensible heat and geopotential flux divergences to those presented in Table 3 for "Europe". The reason may be the much smaller area in Alestalo's work; Europe is not clearly in a climatological jet entrance or exit and the choice of area may then have a drastic impact on the area averaged energetics.

4. CONCLUDING REMARKS

The one-year kinetic energy, sensible and latent heat energy budgets applied over North America, North Atlantic and European regions on the grid point σ level initialized data are in line with the earlier results of e.g. Kung (1967) and Lau (1969) on the regional variations in the time-averaged energy equations.

In the North American area, the climatological jet entrance, there is generation and horizontal flux divergence of kinetic energy and adiabatic heating and divergence of temperature flux in poleward ageostrophic sinking motions in the middle troposphere. The North Atlantic, in the climatological jet exit, is an area of flux convergence and destruction of kinetic energy, adiabatic cooling and convergence of temperature flux, while Europe, not so clearly in a climatological jet entrance or exit, is somewhere between the two extremes. The results reveal a realistic diurnal variation in the energy budget terms due to the thermal tide present in the initialized data.

The residuals of the energy budgets represent the expected sub grid scale effects reasonably well. There is a sharp secondary dissipation maximum at 300 mb level (as a residual) in all three areas. The boundary layer dissipation amounts to about 1.6 w/m² over the continental areas and 2.2 w/m² over the sea. The net heating (as a residual) is about 120 - 130 w/m² in the surface and the heating extends well to the middle troposphere over the ocean area.

The model data, all day 3 forecasts within the year, reproduce the main features but also reveal strong stratospheric cooling, not enough heating in the lower troposphere over the ocean area, spin-up of condensation processes, strong surface friction and weak secondary dissipation maximum in the jet level.

The total energy balance of the earth-atmosphere system obtained for the three areas (as the sum of sensible, latent, kinetic and geopotential energy) is reasonable and points out the relatively large heat transport taking place in the ocean currents.

The good quality of the ECMWF initialized analyses, especially the divergent winds outside tropics, has facilitated the qualitatively and quantitively coherent results presented here for mid latitudes. It may even be possible to map globally the various atmospheric energy flux divergences, and as a side product, the ocean flux divergences, once the remaining problem of weak tropical Hadley circulation as a result of adiabatic normal mode initialization is solved in the ECMWF analysis system.

APPENDIX : Comparison of energy budgets in pressure and sigma coordinate systems

The budget studies are usually based on use of pressure coordinate system. Numerical models tend to have another vertical coordinate, often the normalized pressure or sigma coordinate, because of the lower boundary conditions in the pressure coordinate system. If the predictions are done in one system and diagnostics in another, the vertical interpolations may partially destroy the accuracy needed. Mahlmann and Moxim (1976) showed that errors due to interpolation from sigma to pressure level data and inconsistencies in the calculation of vertical velocity $\omega = dp/dt$ in sigma coordinates resulted in large computational residuals. They derived a more accurate calculation method, but this method gives only the net contribution of flux divergences without the possibility of dividing it into horizontal and vertical parts.

A logical way to avoid these errors is to make the budget calculations on constant sigma levels. Sigma levels may, however, deviate significantly from quasi-horizontal pressure levels over mountainous areas. The interpretation of the energy budget terms on the non-conventional sigma levels may be a problem unless the two systems are compared using identical data. Such a comparison is presented in this appendix, based on a very small sample of 7 cases in February 1976 NMC Data Systems Test objective analyses. The pressure level budget calculations were made in the DST 2.5° grid at 12 pressure levels using the energy equations in pressure coordinate system equivalent to Eqns. (1) - (3) with conventional centred differences calculating by integrating wind divergence vertically from $\omega = 0$ at 50 mb. These calculations were made by Dr. M. Capaldo. The sigma level scheme was the one described in Chapter 4, with the resolution of 15 sigma levels, $\Delta\lambda = \Delta\theta = 1.875^{\circ}$ after interpolations from the 12 pressure levels 2.5° DST data. Both calculations were applied before and after non-linear normal mode initialization. The area considered here is Europe (10° W - 40° E, 35° - 70° N). Because of the small sample and the essentially non-divergent nature of the DST wind analysis (Bergmann et al, 1979), this comparison should be considered only indicative.

Fig. 7 shows the vertical profiles of kinetic energy generation and horizontal flux convergence terms in the two coordinate systems before and after initialization averaged over Europe in the 7 cases. The horizontal flux convergence of kinetic energy is dominated by the advection of upper tropospheric kinetic energy and is rather similar in the two systems. The kinetic energy generation through cross-gradient flow is sensitive to the divergent part of the wind. The vertical profile of this term is similar in the two coordinate systems but its values are smaller in the σ system. Initialization of the data preserves the shape of the profile above the boundary layer but shifts values from

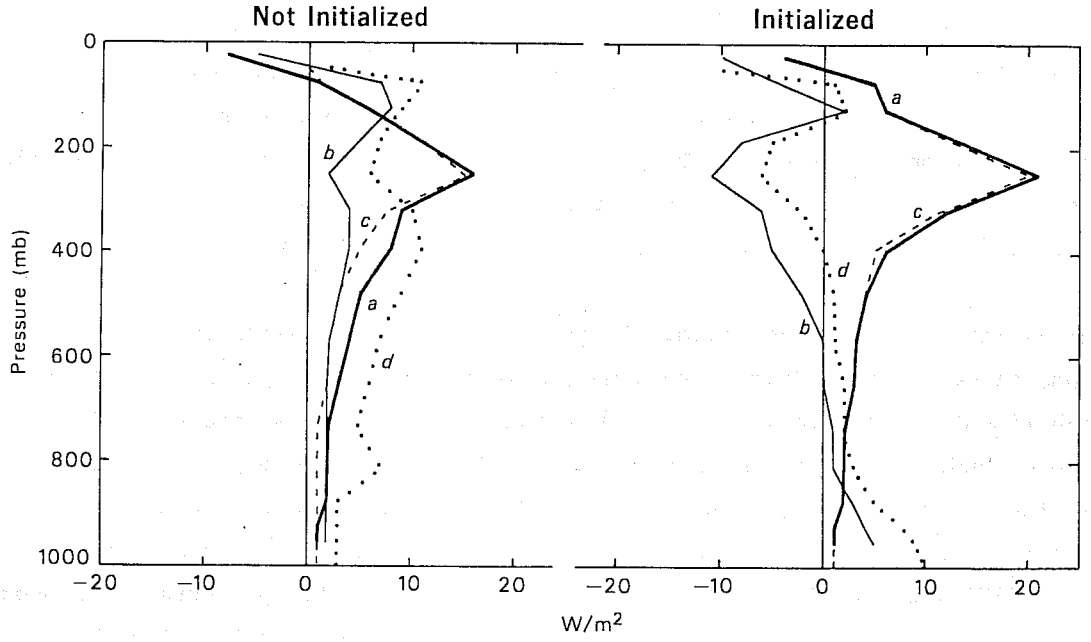

Fig. 7 The kinetic energy generation and flux convergence before and after normal mode initialization in a small sample of NMC analyses over Europe, in sigma and pressure coordinates

a) kinetic energy flux convergence, in sigma coordinates

b) generation, in sigma coordinates

c) kinetic energy flux convergence, in pressure coordinates

d) generation, in pressure coordinates

weak positive to weak negative towards the values obtained on the one-year ECMWF data.

Fig. 8 compares the vertical profiles of conversion $\alpha\omega$. Initialization of the fields reduces the large values towards more reasonable ones, having much more effect in the $\alpha\omega$ values than the choice of vertical coordinate. The fixed boundary value $\omega = 0$ at 50 mb in the p-calculations can be noticed; the boundary conditions $\dot{\sigma} = 0$ at $p = o$ and $p = p_s$ are implicitly involved in the σ system. The diagnostic relation between kinetic energy generation, pressure forces and conversion in the p-system:

$$-\underline{V}.\nabla\phi = -\nabla_p . (\phi\underline{V}) - \frac{\partial}{p}(\phi\omega) - \alpha\omega$$

did not hold when the conventional finite difference scheme was used for each term, the computational residual being of the same order as the smallest term $(-V.\nabla\phi)$. The σ system scheme was constrained to preserve the equivalent diagnostic relation (Eqn. 4), as discussed in Section 3.

Fig. 9 presents the horizontal and vertical humidity flux divergences over Europe in the two coordinate systems. The horizontal flux divergences, dominated by the advective part, are rather similar. The σ system vertical flux divergence shows the expected structure of humidity flux divergence near the surface and convergence in the middle troposphere (upward transport of humidity), but the values are very small. The p-system vertical flux divergence has the same sign everywhere thus failing to integrate vertically to zero as should be the case. The initialization mainly affects the boundary layer values.

The following conclusions are made based on the above results augmented with tests in other areas (Greenland, Atlantic Ocean) with the same data set.

- If the budget terms are not sensitive to small differences in data or calculation methods, the sigma coordinate budget terms are similar to the pressure coordinate budget terms, even in mountainous areas. The interpretation is thus no problem.

- Above the Atlantic Ocean there were less differences between the terms in the two coordinate systems and the effect of initialization is smaller.

- The wind divergence calculation is notoriously sensitive and consequently the results for terms where the divergence is essential (vertical velocity, zonal means of meridional transports, temperature and geopotential flux

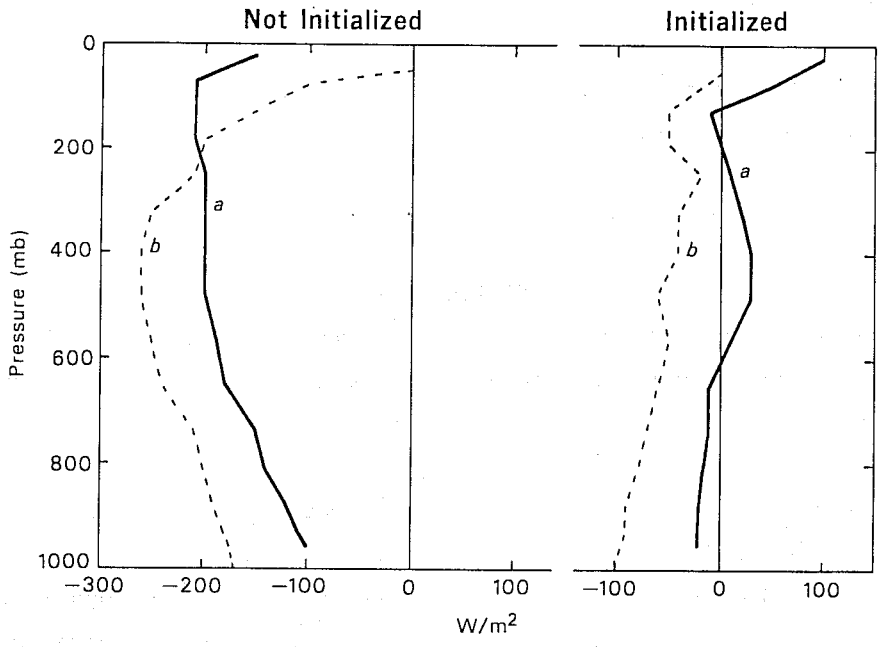

Fig. 8 As Fig. 7 but for the energy conversion $\alpha\omega$

a) $\alpha\omega$ in sigma coordinates

b) $\alpha\omega$ in pressure coordinates

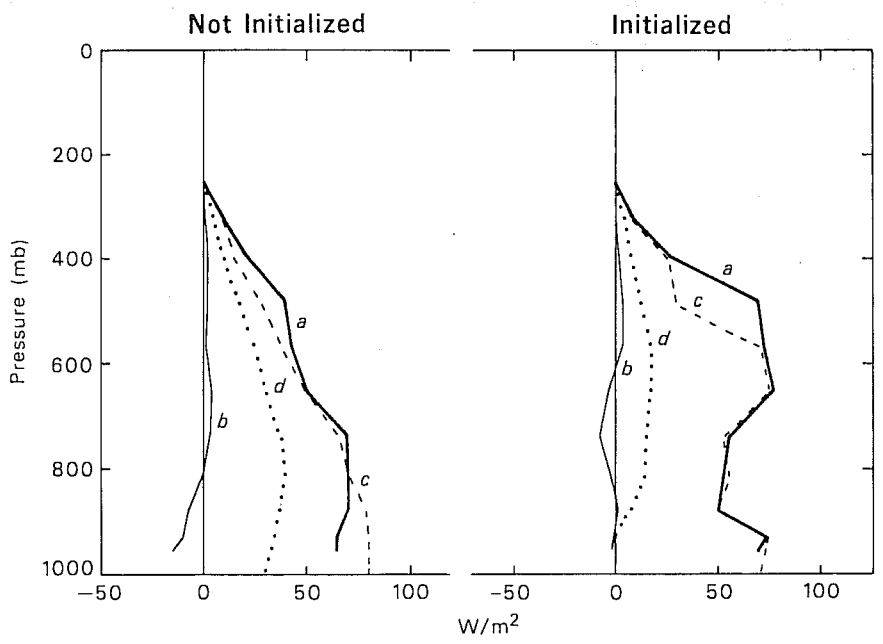

Fig. 9 As Fig. 7 but for the horizontal and vertical latent heat flux convergence

a) horizontal flux convergence, on sigma-coordinates

b) vertical flux convergence, on sigma-coordinates

c) horizontal flux convergence, on pressure coordinates

d) vertical flux convergence, on pressure coordinates

divergences) do differ in the two systems. The σ system results seem to be internally more consistent and physically more reasonable. It is, however, up to the analysis-initialization scheme to catch the correct divergence; in this respect the largely non-divergent DST analyses were not very good for diagnostic purposes (cf. Rosen and Salstein, 1980) and the non-linear normal mode initialization, in trying to create the divergence, has as large or larger effect on the results than the vertical coordinate system.

REFERENCES

Alestalo, M. 1981 The energy budget of the earth-atmosphere system in Europe. Tellus, 33, 360-379.

Bengtsson, L. 1980 Current problems in four dimensional data assimilation. Seminars on data assimilation methods, ECMWF.

Blackmon, M.L., J.M. Wallace, N.-C. Lau and S.L. Mullen 1977 An observational study of the Northern Hemisphere winter time circulation. J.Atm.Sci., 34, 1040-1053.

Burridge, D. 1979 Some aspects of large scale numerical modelling of the atmosphere. Seminars on dynamical meteorology and numerical weather prediction, ECMWF.

Chapman, S. and R.S. Lindzen 1970 Atmospheric Tides D. Reidel Publ. Co., Doidrecht-Holland.

Clapp, P.F. 1961 Normal heat sources and sinks in the lower troposphere in winter. Mon.Wea.Rev., 89, 147-162.

Daley, R. 1980 Normal mode initialization. Seminars on data assimilation methods, ECMWF.

Derome, J. 1981 On the average errors of an ensemble of forecasts. ECMWF Technical Report No.29.

Eliassen, H.-W. 1969 A climatology of Epsilon (Atmospheric Dissipation). Mon.Wea.Rev., 97, 415-423.

Hollingsworth, A., Arpe, K., Tiedtke, M., Capaldo, M., Savijärvi, H. 1980 The performance of a medium range forecast model in winter. Impact of physical parameterization. Mon.Wea.Rev., 108, 1736-1773.

Hollingsworth, A. and Savijärvi, H. 1980 An experiment in Monte Carlo forecasting. Proceedings of the WMO symposium on probabilistic and statistical methods in weather forecasting, Nice, pp.45-47.

Holopainen, E.O. 1973 An attempt to determine the effects of turbulent friction in the upper troposphere from the balance requirements of the large-scale flow: a frustrating experiment. Geophysica, 12, 151-176.

Holopainen, E.O. and Eerola, K. 1979 A diagnostic study on the long-term balance of kinetic energy of the large-scale motion in the atmosphere over the British Isles. Quart.J.Roy.Met.Soc., 105, 849-858.

Holopainen, E.O. and Nurmi, P. 1980 A diagnostic scale interaction study employing a horizontal filter technique. Tellus, 32, 124-130.

Hutchings, J.W. 1957 Water-vapour flux and flux-divergence over southern England: summer 1954. Quart.J.Roy.Met.Soc., 83, 30-48.

Johnson, D.H. 1955 Tidal oscillations of the lower stratosphere. Quart.J.Roy.Met.Soc., 81, 1-8.

Kanamitsu, M. 1980 Some climatological and energy budget calculations using the FGGE III-b analyses during January 1979. Seminars on data assimilation methods, ECMWF.

Kung, E.C. 1967 Diurnal and long-term variations of the kinetic energy generation and dissipation for a five year period. Mon.Wea.Rev., 95, 593-606.

Kung, E.C. and Baker, W.E. 1975 Energy transformations in middle-latitude disturbances. Quart.J.Roy.Met.Soc., 101, 793-815.

Lau, N.-C. 1979 The observed structure of tropospheric stationary waves and the local balances of vorticity and heat. J.Atm.Sci., 36, 996-1016.

Lorenc, A.C. 1981 A global three-dimensional multivariate statistical interpolation scheme. Mon.Wea.Rev., 109, 701-721.

Lorenz, E.N. 1967 The nature and theory of the general circulation of the atmosphere. WMO No.218, TP.115.

Newell, R.E., Kidson, J.W., Vincent, D.G. and Boer, G.J. 1974 The general circulation of the tropical atmosphere and interactions with extratropical latitudes. Vol.2 The MIT Press. 371 p.

O'Brien, J.J. 1970 Alternative solutions to the classical vertical velocity problem. J.Appl.Met., 9, 197-203.

Oort, A.H. and Vonder Haar, T.H. 1976 On the observed annual cycle in the ocean-atmosphere heat balance over the Northern Hemisphere. J.Phys.Oceanogr., 6, 781-800.

Raschke, E. Vonder Haar, T.H., Bandeen, W.R. and Pasternak, M. 1973 The annual radiation balance of the earth-atmosphere system during 1969-1970. From Nimbus 3 radiation measurements. J.Atm.Sci., 30, 341-364.

Rasmusson, E.M. 1968 Atmospheric water vapor transport and water balance of North America. Large-scale water balance investigations. Mon.Wea.Rev., 96, 720-734.

Savijärvi, H. 1977 The interaction of the monthly mean flow and large-scale transient eddies in two different circulation types. Part II: vorticity and temperature balance. Geophysica 14 No.2, 207-229.

Savijärvi, H. 1980 Energy budget calculations and diabatic effects for limited areas computed from ECMWF analyses and forecasts. Proceedings of the Workshop: Diagnostics of diabatic processes, ECMWF, 115-134.

Savijärvi, H. 1981 Energy budget calculations from FGGE analyses and ECMWF forecasts. Proceedings of the International Conference on preliminary FGGE data analysis and results, Bergen, 536-541.

Temperton, C. and Williamson, D. 1979 Normal mode initialization for a multi-level grid point model. ECMWF Technical Report 11, 99pp.

Temperton, C. 1980 Design of the ECMWF normal mode initialization procedure. Seminars on data assimilation methods, ECMWF, 159-193.

Tiedtke, M., J.-F. Geleyn, A. Hollingsworth and J.-F.Louis, 1979 ECMWF model - Parameterization of sub grid scale processes. ECMWF Technical Report 10, 45 pp.

Tiedtke, M. 1980 Diagnostics of diabatic processes in global numerical experiments at ECMWF. Proceedings of the Workshop: Diagnostics of diabatic processes, ECMWF, 135-152.

Vincent, D.G. 1981 The impact of convection on the diagnosis and prognosis of synoptic-scale circulation patterns. Proceedings of the International conference on preliminary FGGE data analysis and results, Bergen, 339-347.

Vonder Haar, T.H. and A.H. Oort 1973 New estimate of annual poleward energy transport by Northern Hemisphere Oceans. J.Phys.Ocean. Vol.3 No.2 169-172.

Wallace, J.M. and F.R. Hartranft, 1969 Diurnal wind variations, surface to 30 kilometers. Mon.Wea.Rev., 97, 446-455.

Wiin-Nielsen, A. 1980 Normal mode initialization - a comparative study. ECMWF Lecture Note No.1.

ECMWF PUBLISHED TECHNICAL REPORTS

No. 1 A Case Study of a Ten Day Prediction

No. 2 The Effect of Arithmetic Precisions on some Meteorological Integrations

No. 3 Mixed-Radix Fast Fourier Transforms without Reordering

No. 4 A Model for Medium-Range Weather Forecasting - Adiabatic Formulation

No. 5 A Study of some Parameterizations of Sub-Grid Processes in a Baroclinic Wave in a Two-Dimensional Model

No. 6 The ECMWF Analysis and Data Assimilation Scheme - Analysis of Mass and Wind Fields

No. 7 A Ten Day High Resolution Non-Adiabatic Spectral Integration: A Comparative Study

No. 8 On the Asymptotic Behaviour of Simple Stochastic-Dynamic Systems

No. 9 On Balance Requirements as Initial Conditions

No.10 ECMWF Model - Parameterization of Sub-Grid Processes

No.11 Normal Mode Initialization for a multi-level Gridpoint Model

No.12 Data Assimilation Experiments

No.13 Comparison of Medium Range Forecasts made with two Parameterization Schemes

No.14 On Initial Conditions for Non-Hydrostatic Models

No.15 Adiabatic Formulation and Organization of ECMWF's Spectral Model

No.16 Model Studies of a Developing Boundary Layer over the Ocean

No.17 The Response of a Global Barotropic Model to Forcing by Large-Scale Orography

No.18 Confidence Limits for Verification and Energetics Studies

No.19 A Low Order Barotropic Model on the Sphere with the Orographic and Newtonian Forcing

No.20 A Review of the Normal Mode Initialization Method

No.21 The Adjoint Equation Technique Applied to Meteorological Problems

No.22 The Use of Empirical Methods for Mesoscale Pressure Forecasts

No.23 Comparison of Medium Range Forecasts made with Models using Spectral or Finite Difference Techniques in the Horizontal

No.24 On the Average Errors of an Ensemble of Forecasts

No.25 On the Atmospheric Factors Affecting the Levantine Sea

No.26 Tropical Influences on Stationary Wave Motion in Middle and High Latitudes

ECMWF PUBLISHED TECHNICAL REPORTS

No.27 The Energy Budgets in North America, North Atlantic and Europe Based on ECMWF Analyses and Forecasts